Journal of Fluids and Structures 17 (2003) 43–55

JOURNAL OF FLUIDS AND STRUCTURES

www.elsevier.nl/locate/jnlabr/yjfls

An experimental investigation of unsteady turbulent-wake/boundary-layer interaction

Z. Gete, R.L. Evans*

Department of Mechanical Engineering, The University of British Columbia, 2324 Main Mall, Vancouver, BC, Canada V6T 1Z4

Received 13 May 2002; accepted 13 May 2002

Abstract

An experimental investigation of unsteady-wake/boundary-layer interaction, similar to that occurring in turbomachinery, has been conducted in a specially modified wind tunnel. Unsteadiness in a turbomachine is periodic in nature, due to the relative motion of rotor and stator blades, resulting in travelling-wave disturbances that affect the blade boundary layers. In the experimental rig, travelling-wave disturbances were generated by a moving airfoil apparatus installed upstream of a flat plate to provide a two-dimensional model of a turbomachine stage. The boundary layer on the flat plate was tripped near the leading edge to generate a turbulent flow prior to interaction with the wakes, and measurements of velocity throughout the boundary layer were taken with a hot-wire probe. The Reynolds number, based on distance along the plate, ranged from 0.144×10^5 to 1.44×10^5, and all data were reduced through a process of ensemble averaging. Due to the nonlinear interactions with the boundary layer, the travelling discrete frequency wakes were found to decrease the shape factor of the velocity profile and to increase the level of turbulent fluctuations. Unlike the phase advance found with stationary-wave external disturbances, velocity profiles subject to the travelling wake fluctuations exhibited increasingly negative phase shifts from the free-stream towards the wall.

1. Introduction

1.1. Unsteady flow in turbomachines

Turbulent boundary layers on turbomachine blades are three-dimensional and highly unsteady. The flow becomes periodically unsteady due to the relative motion of the rotor and stator blades in a stage. A large velocity defect within the wake of an upstream blade generates a varying incidence angle, and a fluctuating velocity at entrance to the next stage. The velocity defect, or wake, travels downstream with a finite speed and intermittently perturbs the boundary layer on downstream blades.

The unsteady interactions of the rotating and stationary blade rows in an axial flow turbomachine affect many aspects of performance such as blade loading, stage efficiency, heat transfer, stall margin and noise generation (Hodson, 1984a, b). However, designers of turbomachinery usually make use of the results of steady flow analysis obtained from cascade tests to develop blade profiles. This procedure is equivalent to assuming that the blade rows of an actual machine are sufficiently far apart so that the flow is steady in both the stationary and rotating frames of reference. Convection of the wakes generated by upstream blades and their interaction with downstream blade rows significantly influences the profile loss compared to that measured in cascade experiments. For instance, the rotor profile loss in a single-stage machine has been found to be between two and four times greater than that for the same cascade model

*Corresponding author.
E-mail address: evans@mech.ubc.ca (R.L. Evans).

0889-9746/03/$ - see front matter
PII: S0889-9746(02)00098-1

operating with steady inlet conditions (Hodson, 1984a). A significant decrease in the stage efficiency estimated from steady cascade data can then be attributed to an increase in profile loss due to the effects of unsteadiness.

On compressor blades the primary concern is with the impact of unsteadiness on aerodynamic performance, while in the case of turbine blades the influence of unsteadiness on the rate of heat transfer to the blade surface is of paramount importance. The response of a row of blades to the free-stream unsteadiness is therefore of fundamental importance in determining the heat transfer and aerodynamic characteristics of the stage. Evans (1975) and Walker (1974) have both shown how wakes were responsible for the unsteady transition process on stator blades located downstream of a rotor row. Early, and fluctuating, transition to turbulent flow was attributed to the wakes impinging on the boundary layer developing on the stator.

Several factors contribute to the generation of unsteadiness in turbomachinery flow, including wakes shed from upstream blades, potential flow interaction due to the relative motion of blades, inlet flow distortions, and rotating stall. In this study unsteadiness due to wake generation and transport, and its interaction with a turbulent boundary layer, were studied in a specially designed experimental rig. These effects were isolated in a two-dimensional model of rotor–stator interaction using linearly traversing airfoils in front of a flat plate in a wind tunnel as shown schematically in Fig. 1. The effects of the convected wakes on the development and characteristics of the turbulent boundary layer developing on the flat plate were then investigated using hot-wire anemometry and an ensemble-averaging technique.

Periodic fluctuations in turbomachines due to wake transport are of the travelling-wave type. In contrast to standing-wave-type free-stream fluctuations that have been quite extensively studied (Karlsson, 1959), travelling waves have a finite wave speed, and result in quite different unsteady effects on the boundary layer. Mathematically, the two types are expressed as follows:

$$U(t) = B\mathrm{e}^{\mathrm{i}\omega t} \qquad \text{standing-wave,}$$

$$U(x,t) = B\mathrm{e}^{\mathrm{i}\omega(t-x/Q)} \qquad \text{travelling-wave,}$$

where U is the velocity, B is the wave amplitude and Q is the wave speed.

1.2. Standing-wave-type free-stream fluctuations

The response of a fully turbulent boundary layer flow to an organised fluctuating upstream or free-stream disturbance has not often been studied at a fundamental level (Carr, 1981). Of those studies conducted, the work of Karlsson (1959) pioneered an experimental investigation of a turbulent boundary layer when the free-stream disturbance was purely time-dependent. This flow disturbance is equivalent to a stationary or standing-wave perturbation to the free-stream flow.

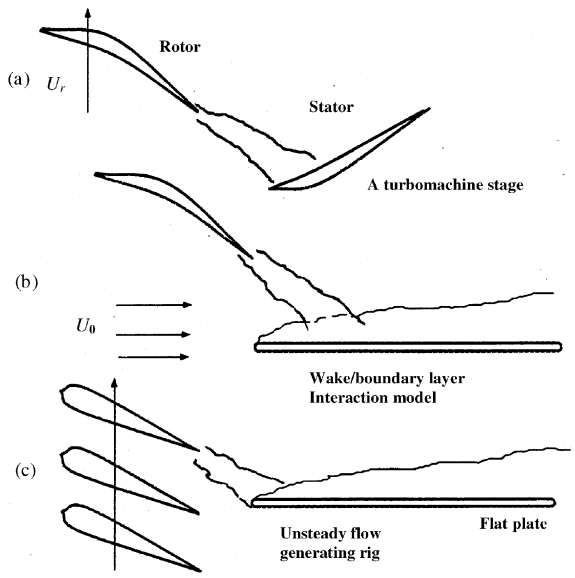

Fig. 1. Simplified physical modelling of a turbomachine stage with a two-dimensional wind tunnel flow.

One of the main conclusions from the unsteady turbulent boundary layer studies concerns the time-averaged mean velocity. The studies conducted by Karlsson demonstrated that the time-averaged mean velocity is nearly invariant, even for high amplitudes and different frequencies of the periodic fluctuations in the free-stream flow. Although the time-averaged mean velocity may suffice in a general and preliminary design procedure, it is important to include the effects of periodicity that are otherwise camouflaged by the time-averaging procedure during the detailed design process. The unsteadiness effects are felt through second-order terms of the free-stream perturbations which are not accounted for in most linearised solution methods (Telionis, 1979, 1981). If the periodic quantities and their interactions with the mean flow are not properly evaluated, the assumption that the mean unsteady velocity is the same as the steady velocity can be misleading.

1.3. Travelling-wave-type free-stream fluctuation

In turbomachinery stages the rotation of blades gives rise to periodic wakes, and the mean-stream flow transports these wakes downstream, where they interact with the boundary layers developing on downstream blades. Despite the widespread existence of travelling-wave free-stream disturbances in turbomachinery, the nature of the wake/boundary-layer interaction and its impact on velocity profiles, phase shift, and losses, is not clearly understood. A fundamental study of unsteady turbulent boundary layers disturbed by a travelling wave was undertaken by Patel (1977). Frequencies in his study ranged from 4 to 12 Hz, the free-stream velocity was 19.8 m/s, and the free-stream amplitude of fluctuations was up to 11% of the mean flow velocity.

Patel (1977) found that the travelling-wave velocity Q influences the response of the boundary layer to the free-stream oscillations. It plays a dominant role in determining whether the boundary layer leads or lags with respect to the free-stream perturbation. However, the mean velocity profile was insensitive to the travelling-wave disturbance. It should be pointed out that the linearisation process employed in the analysis neglected higher order fluctuations which are responsible for the nonlinear interactions in the boundary layer. The linearisation process assumes the decoupling of the oscillations and the turbulence (random fluctuations), restricting the possible interactions with the mean flow.

Evans and Yip (1988) studied a turbulent boundary layer perturbed by convected wakes in the free-stream. Rods mounted on a rotating squirrel cage rotor were used to generate periodic wakes, while a turbulent boundary layer was maintained by tripping the flat plate near the leading edge. A decrease in the shape factor (or increase in the "fullness") of the boundary-layer velocity profile near the wall, compared to the steady flow value, was observed at all stations. The velocity in the inner part of the boundary layer showed a phase lag with respect to the free-stream, and this phase lag increased in the downstream direction due to the lower local convection velocity in the boundary layer that carries the velocity defect of the wake downstream.

2. Experimental apparatus and data processing

2.1. The wind tunnel and rig

A low-speed wind tunnel, together with an unsteady-wake-generating rig, was used to provide a two-dimensional model of a turbomachine stage for this study, as illustrated schematically in Fig. 1. In this model a stator blade is represented by a flat plate located in the tunnel test-section, while a rotor row is represented by a moving cascade of airfoils. The test-section of the wind tunnel has a 400 mm × 250 mm cross-section, and the maximum free-stream velocity is about 20 m/s. Prior to the installation of the unsteady-wake generating mechanism the free-stream turbulence intensity was 0.5%. With the unsteady rig in place, the turbulence intensity increased modestly to about 0.7%.

The unsteady-wake generating rig was installed in the tunnel immediately upstream of the test-section. This moving two-dimensional rotor mechanism consists of two synchronised gear belts to which are attached a series of airfoils which generate periodic wake disturbances in the air-flow just upstream of the flat plate as they pass in front of the test-section. The wind tunnel together with the unsteady two-dimensional rotor rig is illustrated in Fig. 2. A scaled drawing of the flat plate leading edge, hot-wire probe, the trip wire, and the airfoil are shown in Fig. 3.

Seven airfoils were attached across the gear belts so that their vertical plane of motion is perpendicular to the free-stream air-flow entering the test section. The airfoil profile (an NACA 024 blade profile) had a chord length of 50 mm and a span of 390 mm. A stator blade in a real machine was represented by the flat plate where its elliptic leading edge was located 60 mm downstream from the 1/4 chord length of the airfoils (the location at which they are attached to the gear belts). The distance between the airfoil trailing edge and flat plate was on the order of 40 mm. As the system is set in motion, the belt and the airfoils travel with a specified rotor velocity along a vertical plane upstream of the flat plate.

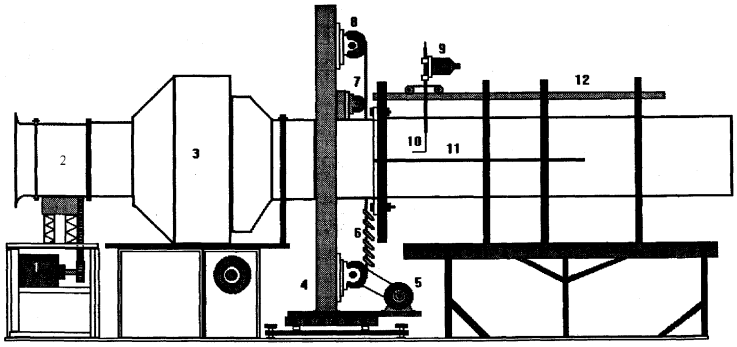

Fig. 2. Wind tunnel and experimental rig. 1.Wind tunnel motor; 2. Fan; 3. Settling chamber; 4. Rig; 5. Rotor drive motor; 6. Airfoils; 7. Gear belt; 8. Gear pulley; 9. Traverse mechanism; 10. Probe and support; 11. Flat plate; 12. Rail.

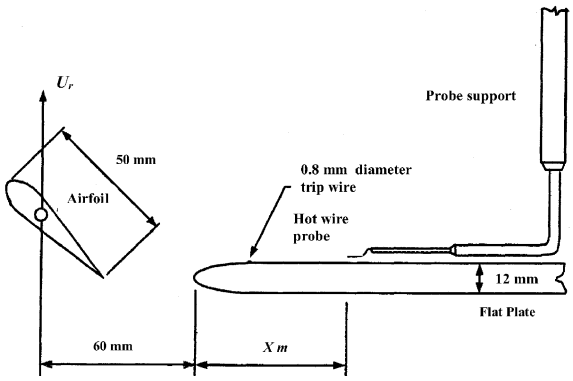

Fig, 3. Schematic of the moving airfoil, flat plate leading edge, and hot-wire probe.

Consequently, the airfoils shed travelling wakes downstream onto the flat plate, in the same way that rotor blades shed travelling wakes onto the stator blades in a real turbomachine.

The choice of seven airfoils in the cascade was made to ensure the periodicity of the travelling wake perturbations on the boundary layer. The periodicity was then verified prior to taking data. The rotor (belt–airfoil system) speed was limited to a maximum of 4.5 m/s, and in the experiments the maximum velocity used was 4.0 m/s. Due to the direction of the shaft rotation, the airfoils travel upwards through the wind tunnel on the downstream side of the rig and travel downwards through the wind tunnel on the upstream side of the apparatus. The distance between the leading edge of the flat plate and the 1/4 chord length of the airfoils at the far upstream side of the rig is 250 mm. The spacing on the belt provides for only a single row of blades to pass in front of the flat plate at any one time.

When the frequencies are normalised with the free-stream velocity and the downstream length x, the reduced frequency ($\varpi = fx/U$), defined as the ratio of (i) the time it takes for a fluid particle of velocity U to travel a distance x to (ii) the time period for the frequency in one cycle, was found to vary from 0.33 to 9.33. This reduced frequency interval was chosen to simulate turbomachine stages that operate in the intermediate reduced frequency range from $\varpi = 1.0$ to 10.0. The undisturbed free-stream velocity, U_0, was set to 3.0 m/s for all experiments. For the simulation to be consistent with a real turbomachine rotor–stator condition, the speed of the airfoils, U_r, was selected to provide a reasonable range of flow coefficient ($C_\theta = U_0/U_r$) from 0.75 to 1.50, as can be seen in Table 1.

2.2. Data acquisition and data processing

A DISA-type 55D10 constant-temperature anemometer was employed along with a single-sensor hot-wire probe (DISA 55P15) to measure all the velocity data. The sensor was a 5 μm diameter platinum-plated tungsten wire with a 2 mm length. All of the data from the hot-wire measurements were acquired with a dedicated 486DX, 50 MHz personal computer. It was equipped with a 12-bit, 32-channel, CIO-AD08 analogue to digital (A/D) converter board. The A/D converter board was configured to accept anemometer output voltages that ranged from 0 to 10 V in 4096 increments.

Table 1
Experimental conditions for velocity measurements: $U_0 = 3.0$ m/s

Case	Rotor velocity U_r (m/s)	Spacing S (m)	Frequency f (Hz)	Station X (m)	Flow coefficient C_θ
1	0.0	—	0.0	0.1, 0.3, 0.5, 0.7	—
2	2.0	0.1	20	0.1, 0.3, 0.5, 0.7	1.50
3	3.0	0.1	30	0.1, 0.3, 0.5, 0.7	1.00
4	4.0	0.1	40	0.1, 0.3, 0.5, 0.7	0.75
5	2.0	0.2	10	0.1, 0.3	1.50
6	3.0	0.2	15	0.1, 0.3	1.00
7	4.0	0.2	20	0.1, 0.3	0.75

It is important to ensure that each data-processing cycle begins at the same time in a period of rotor revolution, and that the same experimental conditions are maintained. A once-per-revolution trigger signal was therefore used to start data registration and acquisition. Data recorded during each set of experiments were processed by the technique of ensemble averaging, as described by Evans (1975), and now commonly known as "triple decomposition". Instantaneous velocity measured in the boundary layer is composed of the time-averaged mean velocity, the periodic fluctuation component due to the periodic wake disturbance, and the random fluctuating velocity component.

The instantaneous velocity u_{ij} at any time in the cycle can be expressed as

$$u_{ij} = \langle U \rangle + u', \tag{1}$$

$$u_{ij} = \bar{U} + \tilde{u} + u', \tag{2}$$

where $\bar{U}$ is the time-averaged mean velocity, $\tilde{u}$ is the periodic fluctuation velocity component, u' is the random fluctuating component, and $\langle U \rangle$ is the ensemble-averaged velocity. Given N number of cycles at any station in the boundary layer, the ensemble-averaged velocity is determined by sampling at constant phase according to

$$\langle U \rangle_i = \lim_{N \to \infty} \frac{1}{N} \sum_{j=1}^{N} u_{ij}. \tag{3}$$

Once the ensemble-averaged velocity is available, the ensemble-averaged turbulent velocity is obtained from

$$\langle u'^2 \rangle_i = \lim_{N \to \infty} \frac{1}{N} \sum_{j=1}^{N} (u_{ij} - \langle U \rangle_i)^2. \tag{4}$$

The time-averaged mean velocity is also calculated by averaging over the number of data points in the ensemble-averaged velocity according to

$$\bar{U} = \frac{1}{M} \sum_{i=1}^{M} \langle U \rangle_i = \frac{1}{MN} \sum_{i=1}^{M} \sum_{j=1}^{N} u_{ij}, \tag{5}$$

where M is the number of data points in the ensemble-averaged quantity. Then the periodic fluctuation velocity component $\tilde{u}$ is determined by simply subtracting the time-averaged mean velocity from the ensemble-averaged velocity.

The phase of the velocity profile across the boundary layer relative to the reference velocity at the free-stream was extracted from the ensemble-averaged velocities at a designated longitudinal location. The time between subsequent airfoil passages is one complete cycle, and is assumed to occupy a phase angle of 360°. Any instant in the cycle is therefore associated with a specific phase angle. Taking the reference free-stream velocity profile to be at 0° phase angle, the phase lead or lag of the remaining velocity records across the boundary layer (at varying vertical distances above the flat plate) follows. The difference in angle between the reference velocity record and that at any vertical position, at the same downstream location, indicates whether there exists a phase lead or lag. A positive angle is indicative of phase lead by the measured velocity record while a negative angle corresponds to a phase lag with respect to the reference velocity record.

3. Experimental results

The term "unsteadiness" in this paper is reserved for a time-resolved flow characterised by periodic fluctuations imposed by an external mechanism. The frequency of disturbance is discrete and small in magnitude when compared to

the random turbulent fluctuations. Various complexities found in a real machine, such as three-dimensional flow, surface curvature, blade entrance angle, blade twist, end-wall effects, secondary flows, etc., were not considered in this study. Instead, attention was paid to conducting a fundamental investigation of the effects of travelling organised fluctuations (wakes in this case) with discrete frequencies on the boundary layer development on a flat plate. The profiles of the wakes ahead of the leading edge of the flat plate were not directly measured, but the time history of the free-stream velocity and hence the wakes have demonstrated the periodic nature of the perturbations. The experimental conditions for the various cases studied are listed in Table 1.

3.1. Steady turbulent boundary layers

To provide a basis for comparison with the unsteady boundary-layer data, several sets of boundary-layer velocity measurements on the flat plate were first taken without the rotor in operation. Fig. 4 provides a comparison of several of the measured steady boundary-layer velocity profiles with both Blasius and one-seventh power law velocity profiles, which are well known in the literature (Schlichting, 1979). The velocities are all normalised with respect to the free-stream velocity. The measured boundary layers are turbulent, except at the $x = 0.1$ m station, where the profile appears to be still transitional in nature. When plotted against y/δ, the profiles did not collapse to a single curve as in the case of laminar boundary layers. This lack of similarity is due to the composite nature of the turbulent boundary layer comprised of the inner and the outer regions. While the inner region contains up to 20% of the total boundary-layer thickness, the outer region covers up to 80% of the entire boundary-layer thickness. The existence of the viscosity-dependent inner part of the turbulent boundary-layer profile and the Reynolds stress-dependent outer part requires different length scales, rendering it difficult to formulate a single dimensionless parameter to collapse the complete velocity profiles into a single curve, as described by Cebeci and Smith (1974).

3.2. Unsteady turbulent boundary layers

3.2.1. Velocity profiles

As the incident wakes from the rotor blades impinge on the turbulent boundary layer on the flat plate, the interaction of the wakes with the boundary layer alters the structure of the velocity profile at each station along the plate. Since the wakes are also travelling with a finite convection velocity in the flow direction, which is somewhat below the mean free-stream velocity, the response of the boundary layer is quite different from the response to stationary waves in the free-stream. The reduced frequency, as noted previously, is an important parameter describing such unsteady flows, and Table 2 shows the values of the reduced frequency for all of the velocity measurements.

Fig. 5 shows phase-averaged velocity profiles at different phase angles in a single period for the cases with reduced frequencies, ϖ, of 0.67, 2.0, 3.33, and 4.67 ($f = 20$ Hz) at stations along the flat plate of $x = 0.1$, 0.3, 0.5, and 0.7 m. These profiles indicate the history and state of fluid motion across the layer as it interacts with the organised disturbances. It is clear from the figures that the boundary layer is sensitive to the external perturbation. The external

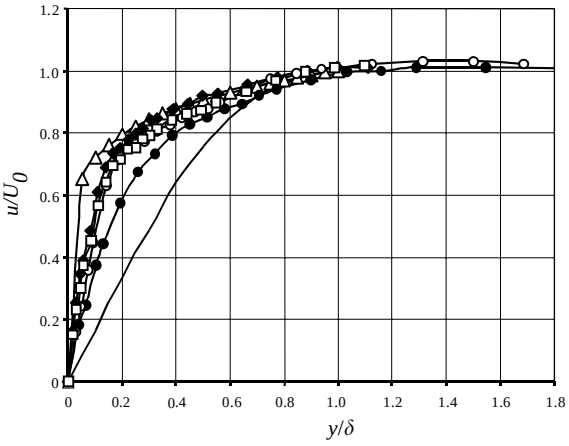

Fig. 4. Comparison of turbulent boundary-layer profiles at constant pressure and zero incidence on flat plate: (——) Blasius profile; (△) 1/7th power law; (●) experiment, $X = 0.1$ m; (○) experiment, $X = 0.3$ m; (◆) experiment, $X = 0.5$ m; (□) experiment, $X = 0.7$ m.

Table 2
Values of the reduced frequency, ϖ

X (m)	$S = 0.1$ m			$S = 0.2$ m		
	20 Hz	30 Hz	40 Hz	10 Hz	15 Hz	20 Hz
0.1	0.67	1.0	1.33	0.33	0.5	0.67
0.3	2.0	3.0	3.99	0.99	1.5	2.0
0.5	3.33	5.0	6.66			
0.7	4.67	7.0	9.33			

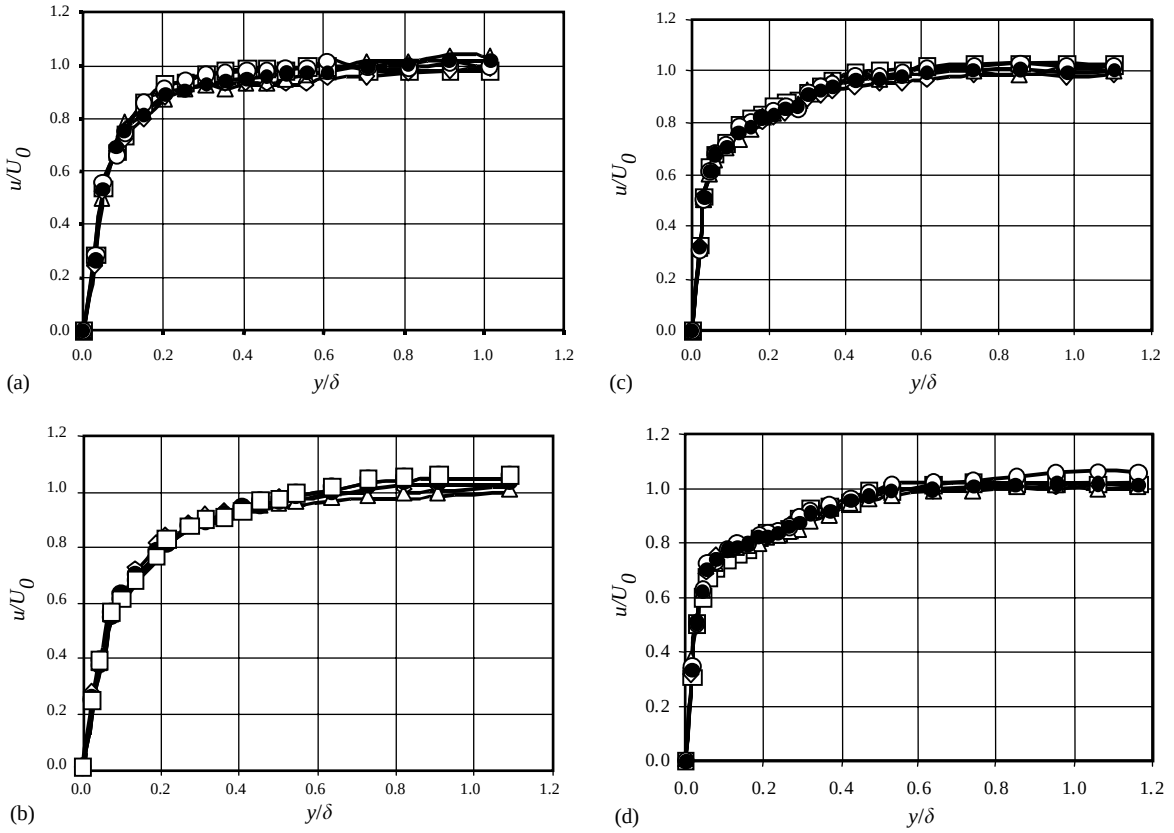

Fig. 5. Velocity profiles at various phases in a single cycle of an unsteady flow, $U_0 = 3.0$ m/s, $U_r = 2.0$ m/s, $S = 0.1$ m, $f = 20$ Hz: (□) 0°; (◇) 120°; (△) 240°; (○) 360°; (●) average. For (a) $X = 0.1$ m; (b) $X = 0.3$ m; (c) $X = 0.5$ m; (d) $X = 0.7$ m.

and internal regions of the turbulent boundary layer react differently throughout the cycle. Ensemble-averaged velocity profile fluctuations in the external region are visibly enhanced in response to the external disturbance, and velocity fluctuations of up to 8% of the free-stream velocity were observed.

It is apparent that the profiles differ significantly at each phase angle. Shear stress diminishes towards the outer region of the profile, and this reduces the influence of viscous forces in the external region and renders it more reactive to the effects of external disturbances. The impressed pressure gradient across the boundary layer appears to cause greater fluctuations in the outer region than it does in the inner region, unlike boundary layers subject to standing waves, in which case the pressure gradient across the layer opposes the inertia forces in the inner region, as described by Karlsson (1959). In this case, however, where there is a travelling-wave disturbance, the pressure gradient reinforces the inertia forces. This phenomenon makes it difficult for the inner region to respond readily, compared to the external region. However, compared to the steady flow velocity profiles, the velocity in the inner region is higher for the periodically disturbed profiles.

The ensemble-averaged velocity profile fluctuations in any cycle diminish with increasing reduced frequency in the downstream direction, where the wakes dissipate their energy as they are convected downstream and more mixing and interaction with the boundary layer takes place. The velocity profiles become fuller along the longitudinal direction, as was observed by Evans and Yip (1988), and this trend increases with increasing reduced frequency. A significant difference between the time-averaged mean velocity profiles, compared to the steady boundary-layer velocity profiles, under similar conditions was observed. Time-averaged mean velocity profiles, obtained from averaging the phase-averaged velocity profiles in a single cycle, are compared to mean velocity profiles for steady flow ($f = 0$ Hz) in Fig. 6. One of the interesting results from this comparison is the increase in the fullness (or decrease in the shape factor) of the time-averaged mean velocity profiles due to the reduced frequency. While the reduction in shape factors is due to the periodic unsteadiness of the flow, the result did not show a linear variation of the profiles or shape factors with increasing reduced frequency. However, the results suggest greater momentum exchange closer to the wall with increasing reduced frequency. There is also clearly a significant difference between the time-averaged mean velocity profiles in unsteady flows compared to the time-averaged mean velocity profiles in steady boundary-layer flows. Previous studies of turbulent boundary layers exposed to standing-wave disturbances (Karlsson, 1959) and boundary layers perturbed by travelling waves (Patel, 1977) showed an insensitivity of the mean boundary-layer profile to frequency. However, the experimental results for the range of reduced frequencies examined in this study show a significant variation in the ensemble-averaged velocity profiles as a function of reduced frequency in unsteady flows.

3.2.2. *Random fluctuations of velocity*

Fig. 7 shows the time histories of the random turbulent fluctuations at transverse locations across the boundary layer ranging from 0.5 to 12 mm for case 2. It is apparent that the impingement of wakes changes the nature and magnitude of the random fluctuations dramatically in the free-stream, as well as across the entire boundary-layer profile. With the

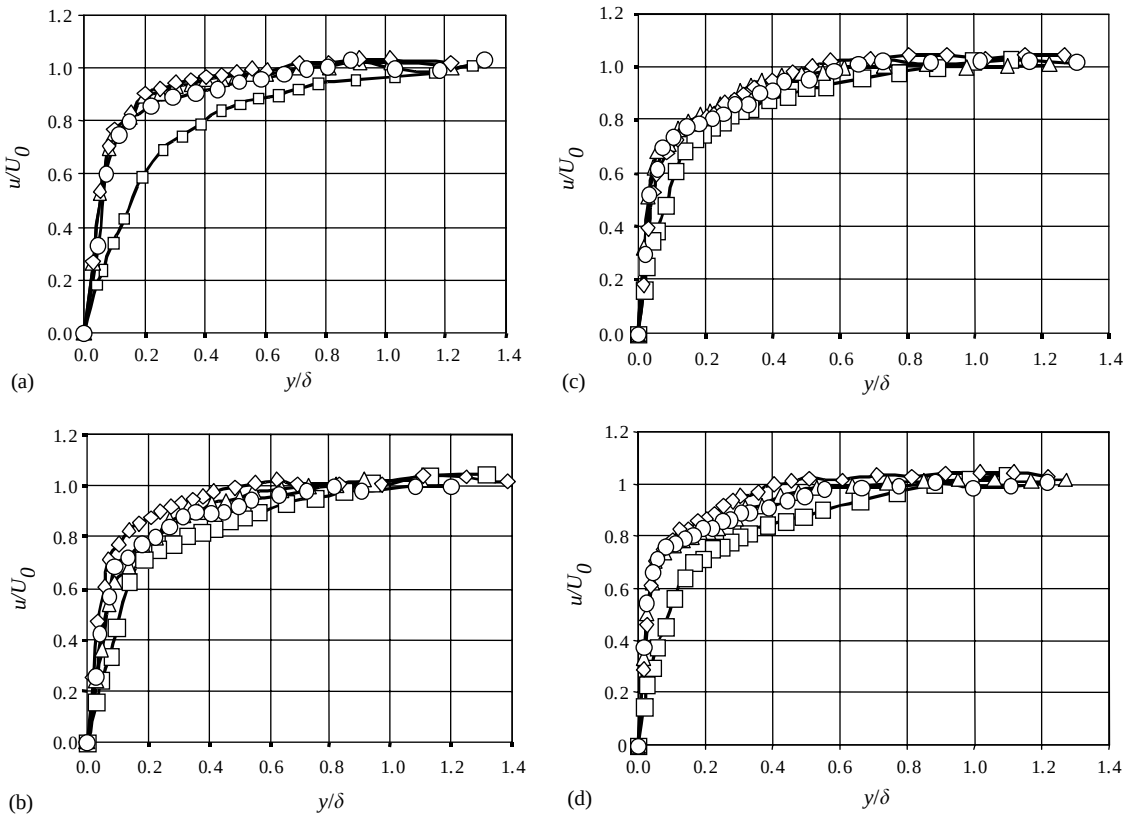

Fig. 6. Comparison of average turbulent boundary-layer velocity profiles for steady and unsteady flows at different frequencies: (□) $f = 0$ Hz, $\varpi = 0$; (△) $f = 20$ Hz, $\varpi = 4.67$; (◇) $f = 30$ Hz, $\varpi = 7.0$; (○) $f = 40$ Hz, $\varpi = 9.33$. For (a) $X = 0.1$ m; (b) $X = 0.3$ m; (c) $X = 0.5$ m; (d) $X = 0.7$ m.

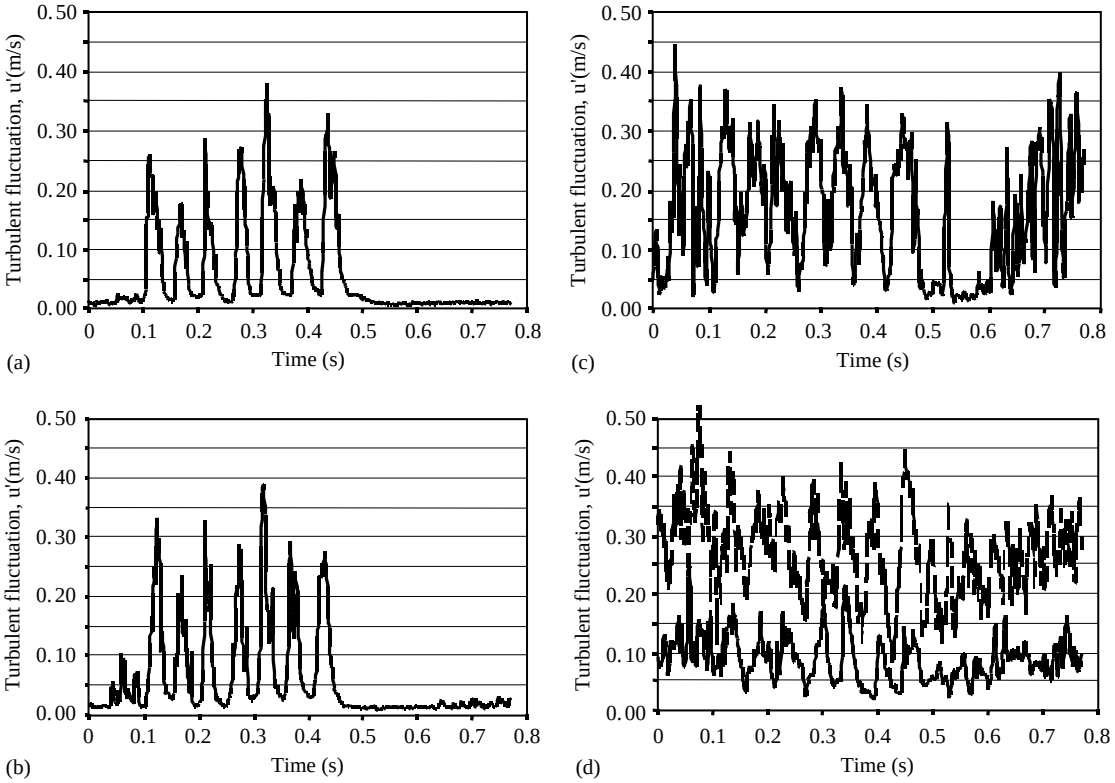

Fig. 7. Time history of the random fluctuations subject to periodic wake disturbances at several transverse locations, $f = 20$ Hz, $S = 0.1$ m, $X = 0.1$ m. For (a) $y = 12$ mm; (b) $y = 8$ mm; (c) $y = 4$ mm; (d) $y = 2$ mm (- - -) and $y = 0.5$ mm (——).

passage of the airfoils in front of the flat plate, the turbulence levels increased more in the outer region than in the inner boundary-layer region.

Ensemble-averaged profiles of random fluctuating velocities at different stations and different frequencies are shown in Fig. 8. The trend of all the profiles is to increase to a maximum near the wall and decrease towards the outer region, as in steady turbulent boundary layers. However, the level of random fluctuations is strongly affected by frequency, tending to increase with increasing frequency. The variation with frequency is much higher in the outer region than in the inner region of the boundary layer. The point of maximum fluctuation for a particular disturbance frequency is also seen to shift towards the wall with increasing distance along the flat plate.

3.2.3. *Velocity phase shift*

The velocity phase shift across the boundary layer is shown as a function of frequency for four downstream stations, and with a blade spacing of 0.1 m, in Fig. 9. It can be seen that the velocity phase lag with respect to the free-stream velocity increases towards the wall in all cases. As a result of mixing and viscous actions in the boundary layer, the identity of a wake profile near the surface of the flat plate is not as distinctive as in the outer region. There is, therefore, a certain degree of uncertainty as to the exact value of the wall phase shift, but is estimated to range from 10% to 15% close to the wall. However, at all reduced frequencies there is a phase lag across the boundary layer.

The phase lag did not show a clear trend with the variation in the reduced frequency at any downstream location along the flat plate. At $X = 0.1$ m, the phase lag appears to span the complete layer from wall to free-stream for all reduced frequencies. At greater downstream distances the phase lag associated with the highest reduced frequency at any station appears to be limited more to the inner part of the boundary layer.

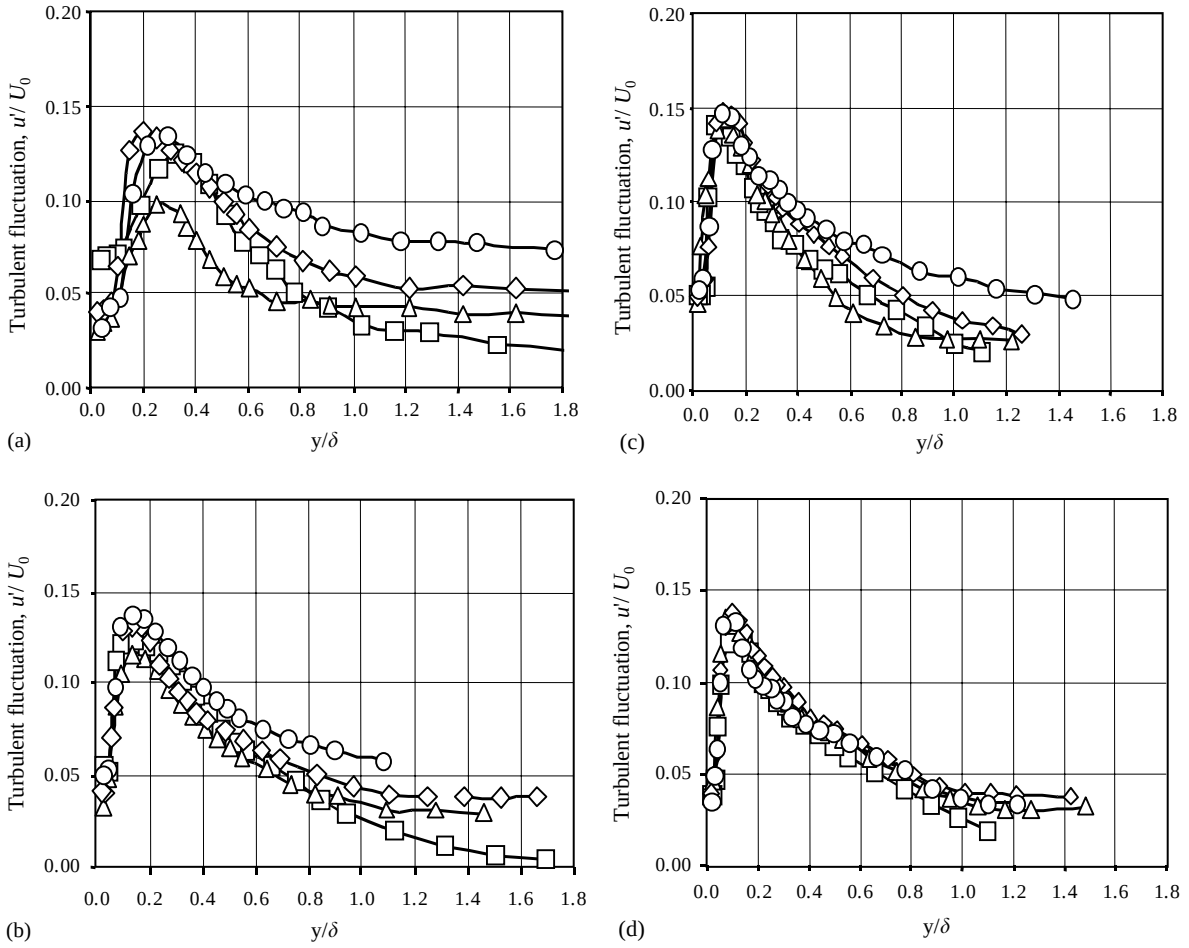

Fig. 8. Profiles of average random fluctuations across the boundary layer at different downstream locations, $U_0 = 3.0\,\text{m/s}$, $S = 0.1\,\text{m}$: (□) $f = 0\,\text{Hz}$; (△) $f = 20\,\text{Hz}$; (◇) $f = 30\,\text{Hz}$; (○) $f = 40\,\text{Hz}$. For (a) $X = 0.1\,\text{m}$; (b) $X = 0.3\,\text{m}$; (c) $X = 0.5\,\text{m}$; (d) $X = 0.7\,\text{m}$.

4. Discussion

Additional terms in the governing equations emerge when a boundary layer develops under the influence of travelling organised fluctuations of discrete frequency. Nonlinear interactions between the time-averaged velocity and the periodic fluctuations, and between the periodic fluctuations and the random fluctuations, provide additional stresses in the flow system. These stresses, similar in nature to the Reynolds shear stress terms, are formed from a correlation of the periodic fluctuations with the mean and turbulent shear stresses and affect the overall structure of the turbulent boundary layer. One of the effects of these additional stresses can be seen in the increased fullness of the average boundary-layer velocity profile and the oscillation of the phase-averaged velocity profiles described previously.

A high level of free-stream turbulence intensity is known to promote turbulence in the boundary layer, as shown by Evans (1985). In a similar way, the presence of a wake disturbance with discrete frequency and amplitude is found to produce increased turbulence levels in the boundary layer. The effect of the intrusion of the wake within the boundary layers is illustrated in Fig. 8, which shows the growth of turbulence intensity with increasing disturbance frequency. For instance, at $X = 0.1\,\text{m}$ from the leading edge of the flat plate the levels of turbulence at the free-stream are 0.7% for the steady flow case (0 Hz), about 4% for unsteady flow with a frequency of 20 Hz, approximately 6% for 30 Hz, and 8% for 40 Hz. Although the influence of the wake turbulence is most visible in the outer region, the effect of the wakes is also felt in the near-wall region. The decay of the turbulence levels with downstream distance is not unexpected, as the wakes dissipate some of their energy as they move downstream along the flat plate.

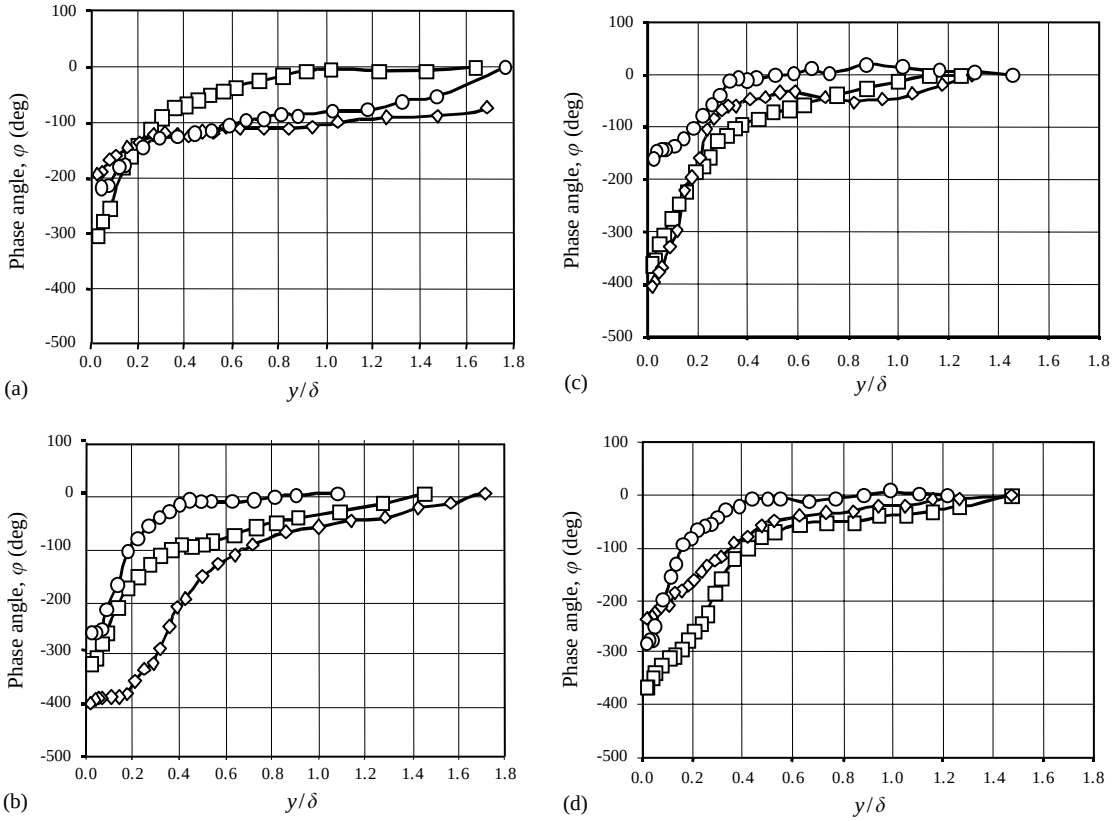

Fig. 9. Phase shift of the unsteady turbulent boundary-layer velocity for various wake passing frequencies at several downstream stations, $S = 0.1$ m: (□) $f = 20$ Hz; (◇) $f = 30$ Hz; (○) $f = 40$ Hz. For (a) $X = 0.1$ m; (b) $X = 0.3$ m; (c) $X = 0.5$ m; (d) $X = 0.7$ m.

The experimental results clearly show that the response of the boundary layer to the external periodic fluctuations is not instantaneous across the profile. Based on the nature of the external disturbance, the boundary layer may react either ahead of time or at a later time relative to the free-stream flow condition. In steady turbulent flows, the mean pressure gradient in the transverse direction, normal to the flat plate, can be assumed to be constant. In unsteady flows, however, the profile is exposed to an oscillating pressure gradient. The frequency of oscillation and convection speed of the externally imposed oscillations are important parameters that affect subsequent development of the unsteady boundary layer. This process is shown by Patel's (1977) analysis of the effects of a travelling-wave like periodic free-stream pressure gradient impressed on the boundary layer.

Let the free-stream velocity be expressed as

$$U(x,t) = U_0 + U_1(x)\mathrm{e}^{\mathrm{i}\omega(t-x/Q)} \tag{6}$$

and the boundary-layer momentum equation for the ensemble-averaged velocity be

$$\frac{\partial u}{\partial t} + u\frac{\partial u}{\partial x} + v\frac{\partial u}{\partial y} = -\frac{1}{\rho}\frac{\mathrm{d}p}{\mathrm{d}x} + \nu\frac{\partial^2 u}{\partial y^2} - \frac{\partial}{\partial y}(u'v'). \tag{7}$$

The free-stream pressure gradient is expressed in terms of the local unsteady acceleration and the convective acceleration as follows:

$$-\frac{1}{\rho}\frac{\mathrm{d}p}{\mathrm{d}x} = \frac{\partial U}{\partial t} + U\frac{\partial U}{\partial x}. \tag{8}$$

Making use of Eq. (6) and performing the proper algebra, the imposed pressure gradient assumes the following form:

$$\frac{\partial U}{\partial t}+U\frac{\partial U}{\partial x}=\mathrm{i}\omega U_1\mathrm{e}^{\mathrm{i}\omega(t-x/Q)}+\left[U_0\frac{\mathrm{d}U_1}{\mathrm{d}x}-\mathrm{i}\omega\frac{U_0}{Q}U_1\right]\mathrm{e}^{\mathrm{i}\omega(t-x/Q)}+\left[U_1\frac{\mathrm{d}U_1}{\mathrm{d}x}-\mathrm{i}\omega\frac{U_1^2}{Q}\right]\mathrm{e}^{2\mathrm{i}\omega(t-x/Q)}. \tag{9}$$

The first term on the right-hand side is the local acceleration. The rest of the terms represent the convective acceleration in the pressure equation.

It is apparent that the magnitude of the travelling-wave velocity, Q, and the amplitude of the fluctuation velocity, U_1, determine the relative importance of the unsteady and convective inertia terms in the above equation. If small-amplitude of oscillation and negligible variation of the amplitude in the downstream direction are assumed, then second-order terms may be neglected. In that case Eq. (9) reduces to

$$-\frac{1}{\rho}\frac{\mathrm{d}p}{\mathrm{d}x}=\frac{\partial U}{\partial t}+U\frac{\partial U}{\partial x}=\mathrm{i}\omega U_1\mathrm{e}^{\mathrm{i}\omega(t-x/Q)}-\mathrm{i}\omega\frac{U_0}{Q}U_1\mathrm{e}^{\mathrm{i}\omega(t-x/Q)}. \tag{10}$$

The terms on the right-hand side are the forces that emanate from the pressure gradient. When inserted into Eq. (7) they interact with the rest of the boundary-layer terms enhancing the phase lead or causing a phase lag in the profile.

The reaction of the boundary layer to the external fluctuating disturbance is dependent on the relative significance of the travelling-wave velocity and the mean free-stream velocity. For large values of Q the second term on the right-hand side of Eq. (10) vanishes. With Q equal to the mean free-stream velocity, all the terms cancel out resulting in a constant-pressure case where there is no effect from the external fluctuations. But, when the travelling-wave velocity is less than the mean free-stream velocity, the convective term becomes significant and tends to increase inertia. The convective term in the pressure gradient is then dominant compared to a purely time-dependent, or stationary wave, perturbation. The effect of the convective term is therefore to add to the inertia term of the momentum equation, forcing the fluid within the boundary layer to lag in phase with respect to the free-stream fluctuations. This phase lag can be clearly seen in the experimental results displayed in Fig. 9.

5. Conclusions

Experimental results have shown that perturbing a turbulent boundary layer with travelling wakes significantly changes the structure of the boundary layer. Not only does it affect the fullness, or shape factor, of the average velocity profiles, but also the magnitude of the random fluctuations. For the external amplitude ratio of 0.10, and Reynolds number range from 0.144×10^5 to 1.44×10^5, the results show that the ensemble-averaged velocity profiles exhibited decreased shape factors ($H\approx1.4-1.5$) compared to those of the corresponding steady velocity profiles ($H\approx1.5-1.7$). The results show qualitative agreement with the decrease in shape factor of the perturbed boundary-layer profile compared to the steady flow values shown in previous work by Evans and Yip (1988), Telionis (1979) and Holland and Evans (1996). The mean of the ensemble-averaged velocity profiles was not the same as the mean steady velocity profile, however, in contrast to both the studies of Karlsson (1959) on unsteady turbulent boundary layers subject to standing-wave-type perturbations and those of Patel (1977) on boundary layers subject to travelling-wave-type disturbances. The results indicate that the use of steady flow data to represent the behaviour of periodic unsteady turbulent boundary layers cannot be readily justified.

Turbulence levels in the boundary layer were found to increase when subjected to external periodic fluctuations in the form of wakes shed from airfoils moving transverse to the flat plate leading edge. For the range of frequency parameter tested, random fluctuation intensities from 4% to 10% were recorded in the free-stream during passage of the wakes for the unsteady cases as opposed to 0.7% for the steady case without wakes. The higher the periodic disturbance frequency, the higher the intensity of the random fluctuations in the boundary layer. Although Patel (1977) observed insensitivity of the random fluctuations to the periodic travelling fluctuations for the cases he considered ($f=4-12$ Hz, and free-stream fluctuations of about $0.11U_0$), the results in this work are qualitatively in agreement with the results of Houdeville et al. (1976). Their investigations, however, were conducted with standing-wave-type free-stream perturbations. Nevertheless, the present results suggest that care should be taken to include unsteady-wake interaction

effects on the Reynolds stress terms in closing the equations of motion when developing computational schemes for unsteady boundary layer development on turbomachinery blading.

Travelling-wave-type fluctuations having a wave speed less than the upstream velocity ($Q/U_0 < 1.0$), and an amplitude ratio of 10%, were found to generate a velocity phase lag with respect to the free-stream across the boundary layer. For the range of reduced frequency investigated experimentally ($\varpi \approx 0.33-9.33$) a velocity phase lag on the order of one period was measured at the wall. Although the phase lag increased towards the wall for any given frequency of disturbance, no clear trend was observed with respect to the effect of reduced frequency on the phase lag.

References

Carr, L.W., 1981. A review of unsteady turbulent boundary-layer experiments. NASA TM-81297.

Cebeci, T., Smith, A.M.O., 1974. Analysis of Turbulent Boundary Layers. Academic Press, London, pp. 1–46.

Evans, R.L., 1975. Turbulence and unsteadiness measurements downstream of a moving blade row. ASME Journal of Engineering for Power 97, 131–139.

Evans, R.L., 1985. Free-stream turbulence effects on a turbulent boundary-layer in an adverse pressure gradient. AIAA Journal 23, 1814–1816.

Evans, R.L., Yip, R.S.K., 1988. An experimental investigation of wake–boundary-layer interaction. Journal of Fluids and Structures 2, 313–322.

Hodson, H.P., 1984a. Boundary-layer and loss measurements on the rotor of an axial-flow turbine. Journal of Engineering for Gas Turbines and Power 106, 391–399.

Hodson, H.P., 1984b. Measurements of wake-generated unsteadiness in the rotor passages of axial-flow turbines. ASME Paper No. 84-GT-189.

Holland, R.M., Evans, R.L., 1996. The effects of periodic wake structures on turbulent boundary-layers. Journal of Fluids and Structures 10, 269–280.

Houdeville, R., et al., 1976. Experimental analysis of average and turbulent boundary-layer. Onera TP No. 30.

Karlsson, S.K.F., 1959. An unsteady turbulent boundary-layer. Journal of Fluid Mechanics 5, 622–636.

Patel, M.H., 1977. On turbulent boundary-layers in oscillatory flow. Proceedings of the Royal Society of London A353, 121–144.

Schlichting, H., 1979. Boundary Layer Theory, 7th Edition.. McGraw-Hill Inc., New York.

Telionis, D.P., 1979. Unsteady boundary-layers, separated and attached. ASME Journal of Fluids Engineering 101, 29–43.

Telionis, D.P., 1981. Unsteady Viscous Flows. Springer, New York.

Walker, G.J., 1974 The unsteady nature of boundary-layer transition on an axial-flow compressor blade. ASME Paper No. 74-GT-135.